

# Characteristics and Evaluation of Water Pollution in the Huanghou Underground River Basin

Caixia YANG \*

School of Karst Science, Guizhou Normal University/State Engineering Technology Institute for Karst Rocky Desertification Control, Guiyang 550001, China

**Abstract** [ **Objectives** ] This study was conducted to investigate water pollution in the Huanghou Underground River Basin. [ **Methods** ] Five representative water quality indicators, ammonia nitrogen ( $\text{NH}_4^+\text{-N}$ ), nitrate nitrogen ( $\text{NO}_3^-\text{-N}$ ), permanganate index ( $\text{COD}_{\text{Mn}}$ ), total phosphorus (TP), and nitrite nitrogen ( $\text{NO}_2^-\text{-N}$ ), were selected. The single-factor pollution index ( $P_i$ ), Nemerow pollution index ( $P_N$ ), and water quality index (WQI) were calculated to quantitatively assess pollution characteristics and evaluate water quality in the basin. [ **Results** ] The overall water quality in the Huanghou Underground River Basin fell within the "slightly polluted to good" range, with pollution primarily concentrated in the upstream areas. The downstream water quality was generally better, as most pollutants from the upstream were diluted or degraded during migration, resulting in little impact on the downstream areas. [ **Conclusions** ] This study provides a theoretical basis for understanding the pollution characteristics and evaluation of water quality in the Huanghou Underground River Basin.

**Key words** Huanghou Underground River Basin; Water body; Pollution assessment; Karst

**DOI:**10.19759/j.cnki.2164-4993.2025.02.016

Water resources are the foundation of human survival. Whether in arid regions with scarce resources or regions relatively abundant in water, water plays an irreplaceable role in maintaining ecosystem stability and supporting human activities<sup>[1]</sup>. However, driven by rapid population growth and accelerated industrialization, water pollution has become increasingly severe worldwide, with water quality showing a continuous decline. Nitrate, as one of the key chemical indicators for assessing water quality, has become a prominent global environmental issue due to its excessive presence in aquatic environments<sup>[2-3]</sup>. In recent years, numerous studies have shown that nitrate concentrations in surface water and groundwater have been increasing year by year, with pollution trends worsening<sup>[4]</sup>. Particularly over the past decade, rapid urbanization, industrial expansion and rising population density have collectively intensified nitrate accumulation in regional water bodies, further challenging the sustainable utilization of water resources<sup>[5]</sup>.

The Huanghou Underground River Basin is a typical karst drainage basin, where water pollution directly impacts local production, livelihoods, and the conservation of the downstream world natural heritage sites. Taking Huanghou Underground River Basin where Libo Karst World Natural Heritage Site is located as the research object, this study aimed to assess the pollution characteristics and spatiotemporal distribution of the water body in the basin. Based on monitoring data of typical pollutants including total nitrogen (TN), nitrate nitrogen ( $\text{NO}_3^-\text{-N}$ ), ammonia nitrogen ( $\text{NH}_4^+\text{-N}$ ), total phosphorus (TP), and organic loads such as

COD and permanganate index, the single-factor pollution index ( $P_i$ ), Nemerow pollution index ( $P_N$ ) and water quality index (WQI) were adopted to systematically analyze variations in pollutant concentrations at different monitoring points in different seasons, so as to identify key pollutant types and reveal the spatio-temporal heterogeneity of water quality as well as the driving factors of pollution.

## General situation of study area

The Huanghou Underground River Basin is located at the border between Guizhou Province and Guangxi Zhuang Autonomous Region, within the coordinates of  $25^\circ 11'$  to  $25^\circ 30'$  N and  $107^\circ 25'$  to  $107^\circ 45'$  E. It represents a typical karst groundwater system in southern Guizhou Province. The area spans Dushan County and Libo County in Guizhou Province, as well as parts of Nandan County in Guangxi, forming a key component of the Dushan karst groundwater system. The study area belongs to a distinctive karst landform unit characterized by fragmented terrain, with dominant geomorphological types including peak-cluster depressions and peak-cluster valleys. The underground karst system is highly developed, with extensive underground rivers and caves. In terms of geological structure, the area is situated at the intersection of three major tectonic zones: north-south, east-west, and northwest-southeast. The region features a dense fault system with intense tectonic activity, where structural fractures and faults significantly influence the storage, flow, and discharge pathways of groundwater. The stratigraphy primarily consists of carboniferous-permian limestone, characterized by hard lithology and strong solubility, providing favorable conditions for the development of karst landforms. It has led to the formation of a complex and typical karst underground river system. The area is rich in fractures, creating highly favorable hydrogeological conditions for precipitation infiltration and groundwater circulation. Although it is a typical

Received: February 3, 2025 Accepted: April 5, 2025

Supported by Guizhou Provincial Key Technology R&D Program (No. 220 2023QKHZC).

Caixia YANG (1995 - ), female, P. R. China, master, devoted to research about physical geography especially karst environment.

\* Corresponding author.

karst mountain area overall, the the karst valleys possess relatively fertile soil and gentle terrain, offering superior natural ecological conditions. Since ancient times, this area has served as one of the important agricultural zones and grain production bases in southern Guizhou<sup>[6]</sup>.

Materials and Methods

Taking Huanghou Underground River Basin where Libo Karst World Natural Heritage Site is located as the research object, this study aimed to investigate and assess the pollution characteristics of the water body in the river basin. Based on monitoring data of typical pollutants including total nitrogen (TN), nitrate nitrogen (NO<sub>3</sub><sup>-</sup>-N), ammonia nitrogen (NH<sub>4</sub><sup>+</sup>-N), total phosphorus (TP), and organic loads such as COD and permanganate index, the single-factor pollution index (*P<sub>i</sub>*), Nemerow pollution index (*P<sub>N</sub>*) and water quality index (WQI) were adopted to systematically analyze variations in pollutant concentrations at different monitoring points in different seasons, so as to identify key pollutant types and reveal the spatiotemporal heterogeneity of water quality as well as the driving factors of pollution. All collected samples were stored in clean sealed containers and immediately refrigerated at 4 °C to prevent biochemical processes from altering water quality characteristics.

Results and Analysis

Load levels of typical pollutants

In this study, five representative water quality parameters were selected: ammonia nitrogen (NH<sub>4</sub><sup>+</sup>-N), nitrate nitrogen (NO<sub>3</sub><sup>-</sup>-N), permanganate index (COD<sub>Mn</sub>), total phosphorus (TP), and nitrite nitrogen (NO<sub>2</sub><sup>-</sup>-N). The single-factor pollution index (*P<sub>i</sub>*), Nemerow comprehensive pollution index (*P<sub>N</sub>*) and water quality index (WQI) were calculated for each parameter to quantitatively assess the pollution status of the river basin.

From the perspective of the mean *P<sub>i</sub>* values, the pollution levels of all parameters were generally. The NH<sub>4</sub><sup>+</sup>-N (0.46) and TP (0.44) showed values closest to the pollution threshold (*P<sub>i</sub>* = 1), but were still classified as "non-polluted" (Table 1). It suggests elevated nitrogen and phosphorus nutrient loads in the area, representing potential pollution risks. The mean *P<sub>i</sub>* value for COD<sub>Mn</sub> was 0.72, indicating that it did not exceed the standard overall. However, some sampling sites in the upper reaches of the basin exceed the standard (from August to November), suggesting that organic matter inputs in certain areas still require attention. In contrast, NO<sub>3</sub><sup>-</sup>-N and NO<sub>2</sub><sup>-</sup>-N showed significantly lower mean *P<sub>i</sub>* values of 0.03 and 0.01, respectively, demonstrating minor pollution risk from nitrate and nitrite nitrogen. That is to say, the concentrations of the two pollutants remain at clean levels in the water body.

As shown in Fig. 1, the *P<sub>N</sub>* values further revealed the comprehensive pollution status. The results demonstrated that the pollution levels in the upstream areas were significantly higher than those in the downstream areas. In the upstream section, water quality ranged from clean to severely polluted. In specific, clean

samples and relatively clean samples accounted for 7.0% and 19.2%, respectively, and lightly polluted samples, moderately polluted samples and severely polluted samples accounted for 50.9%, 8.8% and 14.0%, respectively. The elevated pollution levels upstream may be associated with agricultural runoff, domestic sewage, and tourism-related discharges. Furthermore, the upstream areas exhibited higher pollution levels during the dry season, likely due to reduced river flow and consequently weaker self-purification capacity. In the downstream section, the vast majority of water samples fell within the clean to lightly polluted range, indicating overall better water quality. It suggested that pollutants from upstream underwent significant dilution and degradation during migration, resulting in little effect on downstream areas.

Table 1 Calculation results of *P<sub>i</sub>*

Index	NH <sub>4</sub> <sup>+</sup> -N	NO <sub>3</sub> <sup>-</sup> -N	COD <sub>Mn</sub>	TP	NO <sub>2</sub> <sup>-</sup> -N
Mean <i>P<sub>i</sub></i> value	0.46	0.03	1.35	0.44	0.01

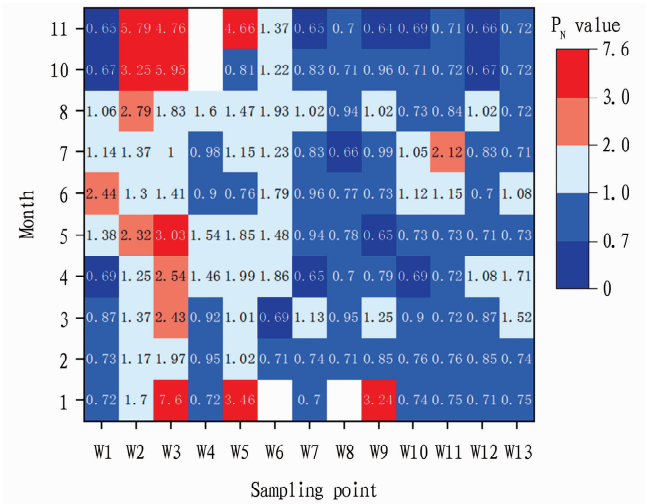


Fig. 1 *P<sub>N</sub>* distribution at various sampling points in different periods

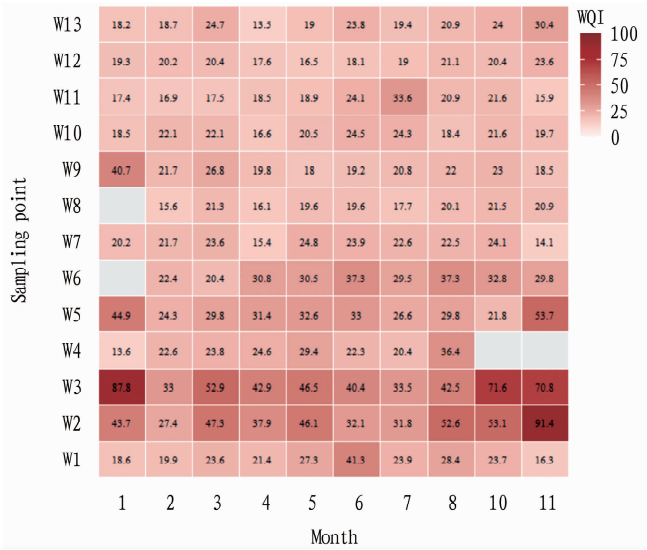


Fig. 2 Distribution map of water quality index at different sampling points in different periods

## Water quality index levels

The water quality index (WQI) was calculated for various monitoring sites in different months using a multi-parameter weighting method. The WQI values were classified into five grades: excellent water quality ( $WQI < 50$ ), good water quality ( $50 \leq WQI < 100$ ), poor water quality ( $100 \leq WQI < 200$ ), very poor water quality ( $200 \leq WQI < 300$ ), and water unsuitable for drinking ( $WQI \geq 300$ ). Fig. 2 shows the heatmap for monthly WQI distribution at various sampling points throughout the year.

The overall distribution results indicated generally good water quality conditions in the study area. Statistical analysis revealed that 90.77% of samples fell into the "excellent water quality" category, demonstrating that the vast majority of sampling points maintained safe water quality indexes in different seasons. Samples classified as "good water quality" accounted for 6.15% and were primarily concentrated at local monitoring points such as W2 and W3, reflecting the local time periods of pollution interference. Notably, no samples were categorized as "poor water quality" or worse, indicating that the underground river system maintains strong environmental carrying capacity under current climatic and land-use conditions. Additionally, the data missing ratio was 3.08%, primarily caused by sampling vacancies due to equipment failures at individual sampling points or extreme rainfall/drought conditions, which did not significantly affect the representativeness of the assessment results.

The figure further reveals that monitoring points W2 and W3 represented high-value zones, frequently exhibiting WQI values  $> 50$  (classified as "good water quality"). Notably, some monthly values approached or exceeded 90 (*e.g.*, W3 in January, May, and November; W2 in November). These elevated values might be correlated with point-source pollution from domestic wastewater discharge, transportation hubs, or high-density tourist areas upstream. Point W5 also showed a mild water quality decline ( $WQI = 53.7$ ) in November, suggesting certain organic matter accumulation or non-point source scouring residue during the post-flood season.

Temporally, some monitoring points showed slightly elevated WQI values during the rainy season (May–October), suggesting that stormwater runoff or surface flow may enhance pollutant transport into the underground river system. Particularly during August–November, significant water quality fluctuations at W2 and W3 indicated potential risks arising from combined effects of rainfall and land-use changes. In contrast, other monitoring points (W11–

W13) in hydrologically stable mid-downstream areas maintained excellent water quality throughout the year, with WQI consistently below 30.

## Conclusions and Discussion

The results of single-factor pollution index demonstrated that TP,  $NH_4^+-N$ ,  $NO_3^--N$  and  $NO_2^--N$  maintained clean levels overall, while  $COD_{Mn}$  exhibited certain organic pollution characteristics. The Nemerow index analysis revealed that the upstream pollution was greater than the downstream pollution. In upstream areas, the water quality ranged from clean to severely polluted, with lightly polluted samples predominating (50.9%), and the downstream samples were mainly within clean to lightly polluted levels, indicating overall better water quality and limited upstream pollution impacts on downstream areas.

The multi-index evaluation involving WQI demonstrated generally favorable water quality conditions in river basin, with over 90% of samples classified as "excellent water quality". Local water quality deterioration was observed only at upstream monitoring points including W2 and W3 during late rainy seasons or low-water periods, revealing vulnerabilities driven by land use and precipitation in specific areas.

In summary, the Huanghou Underground River Basin maintained overall water quality within the "slightly polluted to good" range, and the pollution was primarily concentrated in upstream areas.

## References

- [1] NOREEN BEG, MORLOT JAN-CORFEE, DAVIDSON OGUNLADE, *et al.* Linkages between climate change and sustainable development[J]. *Climate Policy*, 2002, 2(2): 129–144.
- [2] NICOLAS GRUBER, GALLOWAY JAMES-N. An Earth-system perspective of the global nitrogen cycle[J]. *Nature*, 2008, 451(7176): 293–296.
- [3] MA CM, ZHAO LH, LIU CF, *et al.* Advances of the research of isotopic analysis technology for nitrate in natural water[J]. *Geotechnical Investigation & Surveying*, 2010, 38(7): 37–41. (in Chinese).
- [4] BATSAIKHAN UURIINTUYA, ZSOLT DARVAS, RAPOSO. People on the move: Migration and mobility in the European Union[J]. *Archive of European Integration*, 2018, 190.
- [5] PACHECO FAL, SANCHES FERNANDES LF. Environmental land use conflicts in catchments: A major cause of amplified nitrate in river water [J]. *Science of The Total Environment*, 2016: 548–549.
- [6] LI JY. Basic characteristics of formation and development of karst underground water system in Dushan, Guizhou[J]. *Journal of Guizhou University of Technology*, 1981(3): 77–95. (in Chinese).

Editor: Yingzhi GUANG

Proofreader: Xinxiu ZHU

(Continued from page 79)

- [7] LAMRANI MA, BOULARD T, ROY JC, *et al.* SE—structures and environment: AirFlows and temperature patterns induced in a confined greenhouse[J]. *Journal of Agricultural*, 2001, 78(1): 75–88.
- [8] CHENG JCP, KWOK HHL, LI ATY, *et al.* Sensitivity analysis of influence factors on multi-zone indoor airflow CFD simulation[J]. *Science of The Total Environment*, 2021, 761: 143298.

- [9] VAN HENTEN EJ, BONTSEMA J, VAN STRATEN G. Improving the efficiency of greenhouse climate control: An optimal control approach [J]. *Quarterly Journal of the Royal Netherlands Society for Agricultural Sciences*, 1997, 45(1).
- [10] DONGDONG MA, NEAL CARPENTER, HIDEKI MAKI, *et al.* Greenhouse environment modeling and simulation for microclimate control[J]. *Computers and Electronics in Agriculture*, 2019, 162: 134–142.

Editor: Yingzhi GUANG

Proofreader: Xinxiu ZHU